

May, 1975

SOME EARLY RESULTS FROM A SEGMENTED CALORIMETER^{++,+++}

FNAL^{*} - LEHIGH^{**} - PENN⁺ - WISCONSIN^{**} Collaboration

A. Erwin^{**}, E. Harvey^{**}, A. Kanofsky^{**}, W. Kononenko⁺, T. Kondo⁺,
L. Kroger⁺, R. Loveless^{**}, W. Selove⁺, F. Turkot^{*}, D. Winn^{**},
B. Yost⁺. Report given by W. Selove

⁺⁺ Contribution to the Calorimeter Workshop, Fermilab, May 9-10, 1975.

⁺⁺⁺ Work supported by U.S.E.R.D.A.

We report here some very early results from test measurements at FNAL finished two weeks ago.

The system with which these measurements were made is shown in Figure 1. The calorimeter design is modular in area and in depth. The modules use steel plates in liquid scintillator, except for box A, where Pb plates are used⁽¹⁾. The 4 boxes are each subdivided optically into four segments, each 1 foot square. Light is collected by a set of fluorescent bars⁽²⁾, indicated schematically in Figure 2. This scheme has the virtue of giving relatively uniform light collection with a quite small final cross section of light pipes. The amount of light obtained is of course much smaller than the ultimate amount obtainable directly from scintillator, but is nevertheless quite substantial. Tollestrup has reported that the CalTech gamma hodoscope gives about 100 photoelectrons per GeV for electromagnetic showers. The present system gives 1/4 to 1/3 as much, in box A.

This calorimeter development is for NAL experiment 246, a study of high p_T events. For such a study, it is necessary to have energy resolution of at least a certain critical quality, or else the

-
- (1) The steel plates are about 1 inch thick, with 1 inch gaps; the Pb plates are 1/4 inch thick, with 1 inch gaps. The total thickness of the array is 9 collision lengths.
- (2) G. Keil, Nuc. Instr. & Meth. 83, 145 (1970), and 87, 111 (1970).

steep p_T dependence of the produced events will create an unworkable spectrum unfolding problem. Specifically, the high energy tail of the pulse height spectrum must not stretch out too far, or else events of a given p_T will simulate the much less frequent events of a substantially higher p_T . We found in early work with a test calorimeter that we could obtain a major improvement in tail sharpness for low particle energies, 10 GeV and lower, by using a large "sampling fraction" (fraction of total cascade energy deposited in the active medium^(3,4)). Since the calorimeter system for E-246 is to be quite large in area, we have chosen to work with liquid scintillator for economic reasons.

Before presenting some of our present results, we make remarks on two matters. (1) PM gains were balanced roughly, before taking the data we report, by using traversing muons. Final resolution may improve somewhat when the gains are adjusted and the pulse-height spectra re-calculated. (2) We encountered a problem with spurious signals produced in the glass end window and side walls of the photomultipliers (6342A/V1). We found in our measurements that the cascade shower produced by a particle of say 50 GeV has a substantial fraction of the energy in a very concentrated core, of diameter less than one inch. When this core passes through the PM end window, Cerenkov light is produced and gives a spurious signal -- up to 200 photoelectrons per traversing shower particle when the particle passes

(3) Turkot, et.al., U. of Pa. internal report, 1973.

(4) Gabriel, this workshop.

edgewise through the end window. Particles passing perpendicularly through the end window give 10 to 20 photoelectrons per particle. We expect to remove even this level of signal by the use of a new tube, which RCA is building, which will have a separate internal cathode, not in contact with the end window.

Data were taken with a particle beam entering the array of Figure 1 normal to the face. Entering location was varied, to provide information on shower size and on some edge effects. Most of the results shown below were taken with the entrance location 3 inches to the right of center and 3 inches below; further below, we give results from some horizontal scans taken with a beam entering 3 inches below the dividing partition.

Figure 3 shows the pulse height spectrum (sum of ADC's for all 16 PM's) for 100 GeV π^- . Only a preliminary adjustment of the relative PM gains has been made for this plot and the following ones, following a brief study of the results; only the gain of the B tubes has been adjusted.

Most of the signal, for the previous plot, comes from segment 4 (see Figure 1). The pulse height spectra for this segment, for the individual A B C D boxes, are shown in Figure 4. In Figure 4a, for segment A4, evidence can be seen of a small residual contamination of 100 GeV/c electrons in the beam -- the beam Cerenkov counter did not give perfect veto-ing of such electrons.

Figure 4a also shows that in the front box (17r1 and 1.3 absorption lengths) 100 GeV/c-pions frequently deposit a large fraction of their total energy.

Similar data were taken for energies from 20 to 200 GeV. No deviation from linearity was found to an accuracy of a few percent.

In Figures 5 to 7 we show some results for 40 GeV. Figure 5 shows the spectrum for 40 GeV e^- . The FWHM in this plot is 15%. Figure 6 shows a corresponding plot for 40 GeV/c pions. As we will discuss further below, it is possible to improve the resolution for these data by using a weighting procedure, giving more weight to those segments outside of the segment where the beam enters. Such a weighting procedure was described by Rehak in a report in this workshop yesterday. In our own work we also found that such weighting could give improved resolution. As an example of the effect of such weighting we show in Figure 7 the re-calculated data from Figure 6 using a weighting procedure in which we assign the signal from segments 1, 2, and 4 a relative weight two times as large as for segment 4 (which is the segment where the beam enters). This particular weighting gives a FWHM of 30%, compared to the value of 37% for the unweighted sum.

This weighting procedure is useful in trying to understand the mechanism of energy deposition and of spread of pulse heights, and might be useful to improve the resolution of a detector which has to respond

to a single particle at a time. It seems less likely that such a technique could be used to improve resolution in an experiment like E-246, which is specifically designed to look at multi-particle events.

The reason why the weighting procedure improves the resolution can be readily understood by looking at the detailed energy deposition pattern of individual events. From event to event the fraction of the energy which is deposited as electromagnetic showers, from π^0 's, varies considerably. When a major part of the energy of the incoming particle is converted to π^0 's, the resulting electromagnetic shower is then absorbed within a relatively short distance in the calorimeter; there is negligible escape out the back, and, more relevant, negligible energy deposition at transverse distances more than a few inches from the entering beam line. On the other hand, when most of the cascade energy is deposited in non- π^0 form, then some substantial number of nuclear stars is formed, the total energy available to produce a light signal is smaller, and at the same time a relatively larger amount of energy is deposited at larger transverse distances from the entering beam line. Thus the detection of substantial amounts of energy at large transverse distances is indicative of two effects. First, a relatively larger amount of energy has been used for nuclear breakup and so is not available to produce a light signal. Moreover, nuclear breakup also

produces larger numbers of particles of low energy, which give reduced signal because of saturation effects in the scintillator. Second, for events with large transverse spread more energy is likely to escape out the sides of a calorimeter of limited transverse dimensions. Both these effects can be crudely partially compensated by such a weighting procedure as described above. A major implication of this explanation is that a substantial amount of energy loss through side escape of cascade fragments probably occurs in the present array. As Frank Sciulli has reported in his talk at this workshop, a relatively small amount of escape energy can produce a substantial broadening of resolution.

The detailed deposition pattern of individual events gives support to this picture. We have studied this deposition pattern in a preliminary fashion, particularly looking for correlations between the nature of the deposition pattern and the total pulse height for individual events. In Figure 8 we show a sketch of the pulse height spectrum for 100 GeV/c pions, corresponding to Figure 3 above. We have selected events in several different regions of the pulse height spectrum, indicated in Figure 8 as groups 1, 2, and 3. (The total number of events in this run was 10,000.) For events near the central peak (group 2), the deposition pattern is of course not exactly the same from event to event. Yet there is a general overall character for these events, and that character is indicated in Figure 9. The individual numbers correspond roughly to the number of GeV signal

coming from each of the 16 PM's. Figure 10 shows the typical deposition pattern for events with total pulse height substantially above the average value (group 3). In these events, typically a major fraction of the energy is deposited in the A box. The A box is only 1.3 absorption lengths thick. To deposit such a large fraction of the energy in this box requires that in the first collision by the entering particle, a major fraction of the total energy is converted into π^0 's. That event will then have less pulse height loss due to the several effects of binding energy, saturation of light output for slowly moving nuclear particles, and escape out the sides or back.

For the events which give total pulse height appreciably smaller than the peak pulse height (group 1), the events are much less similar from event to event. Two typical events of this kind from a modest sample are shown in Figure 11. Although these events are quite dissimilar, they, and other events in that region of the pulse height spectrum, share one feature in common. Namely, the energy deposition shows a much larger spread than the average event, usually transversely, and sometimes also longitudinally.

To try to show more clearly the relative transverse spread of signals of different total pulse height, we sum all four boxes, segment by segment, and show the deposition pattern as seen looking

into the face of the calorimeter array. At the bottom of Figure 11 we see that for these two events approximately 67% of the total energy is deposited in segment 4, and 33% in segments 1, 2, and 3. Similar summaries are shown in Figure 12 for 4 different cases. (For electrons, only 3 GeV of the total of 100 GeV penetrates beyond box A.) In this figure we thus see the collected results showing a strong correlation between transverse spread and total pulse height. Not shown in this report but also seen by us, and by a number of other workers, is a strong correlation also between the longitudinal deposition pattern and the total pulse height. These various correlations may make it possible, by a later treatment, to improve the resolution.

Finally, we show in Figures 13-15 a few results on uniformity and on shower size. In Figure 13a, we show the peak pulse height for the ADC sum, for a horizontal traverse of the entering beam position. The point $x = \text{zero}$ is the location of the partition between the left half and the right half of the array. (The beam was kept 3 inches below the array center, during this traverse.) Except near the edge, the response is uniform to a few percent.

We note that this uniform response does not mean that there is negligible leakage. Information on the probable amount of leakage, as well as detailed information on the radial distribution of energy

deposition (averaged over many events), is shown in Figure 13b for the same data. Figure 13b shows that the major edge effect in Figure 13a is well reproduced by the division of energy between left and right halves as we move across the divider, but Figure 13b also gives a useful measure of how much energy is deposited across a divider 6 inches or more from the entering beam line.

The energy deposition past such a divider, and more generally the energy deposition per "slice in x" -- the projected transverse energy deposition -- is shown in Figure 14 for the same data. Here one sees that for the present geometry an appreciable amount of energy is deposited at distances of 6 inches and more from the beam line. This is true for the average event -- for individual events the transverse deposition of course varies greatly.

Figure 14 also shows clearly the very concentrated "core" in the average 200 GeV shower. Approximately one third of the total energy deposition is in a central core of less than one inch diameter. This result implies that even in collisions with the heavy nuclei in this array, the typical π^0 production in the cascade involves initial production of a relatively small number of high energy π^0 's. Because of this concentrated core, a calorimeter for use in high- p_T studies must have no localized areas of unusually large response.

Figure 15 shows similar measurements for 20 GeV, pions and electrons. Even at this energy, pions show a relatively concentrated core in the cascade.

We thank warmly the many people at our institutions who have helped in the construction of this equipment, and Fermilab for arranging for these measurements.

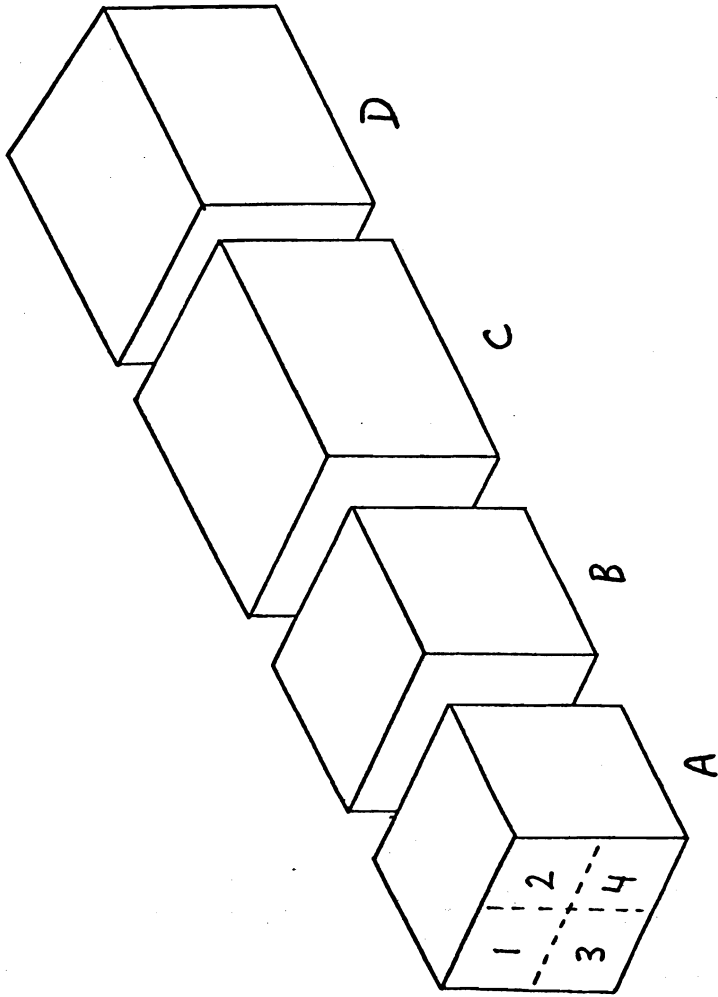


FIG. 1

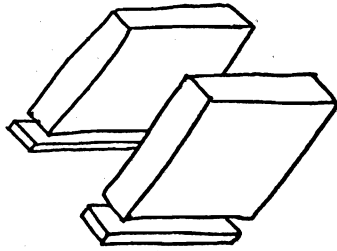
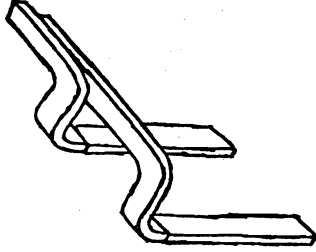


Fig. 2

100 GeV/c π^-

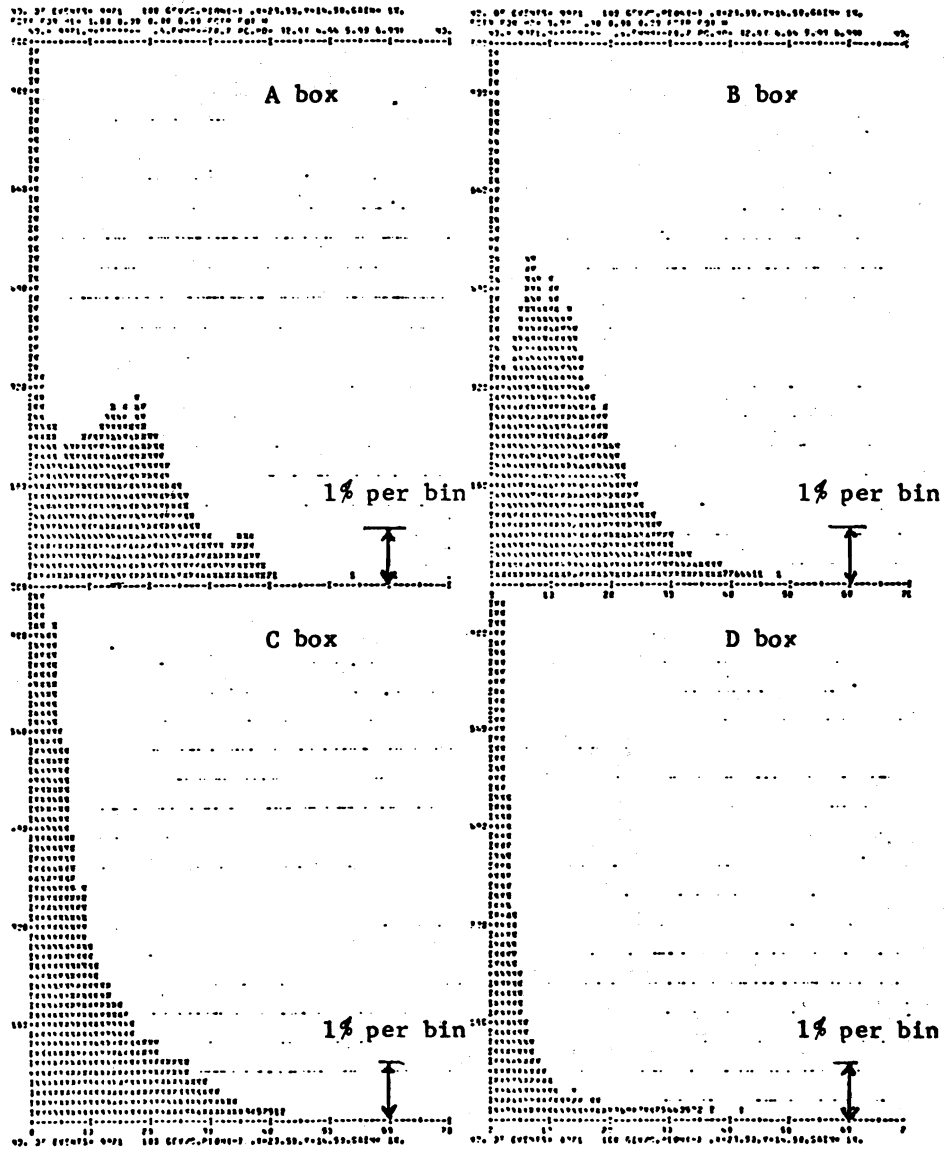


Fig. 4

40 GeV/c ELECTRON

FWHM = 15 %

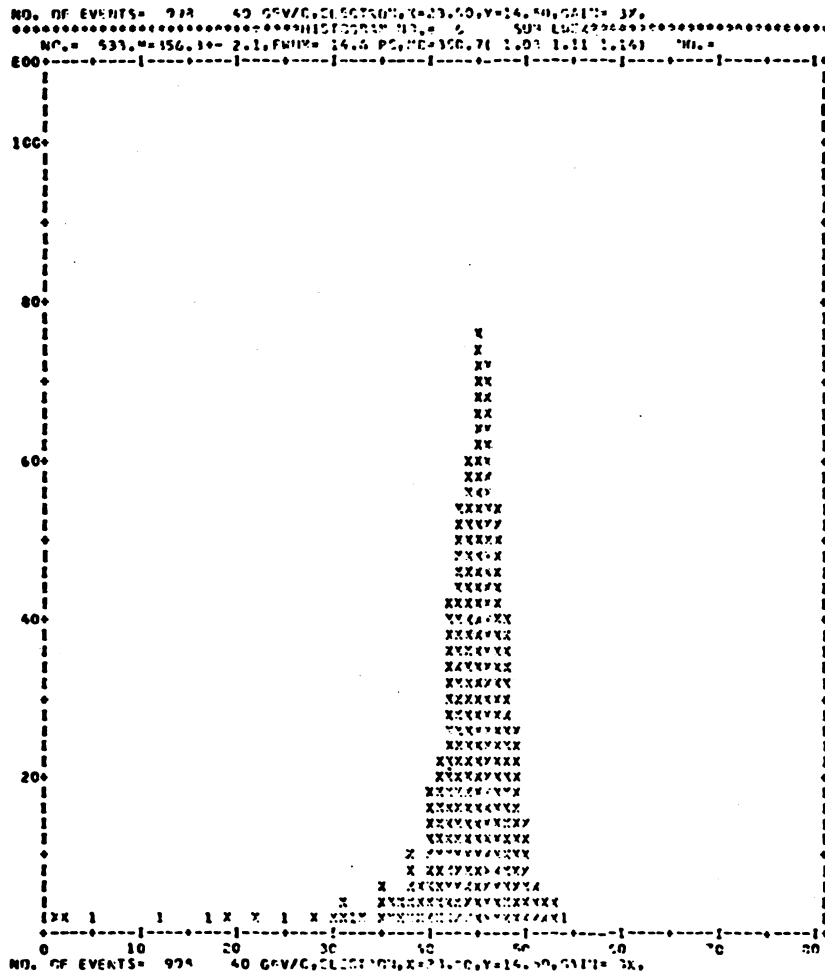


Fig. 5

40 GeV/c PION(-) FWHM = 37 %

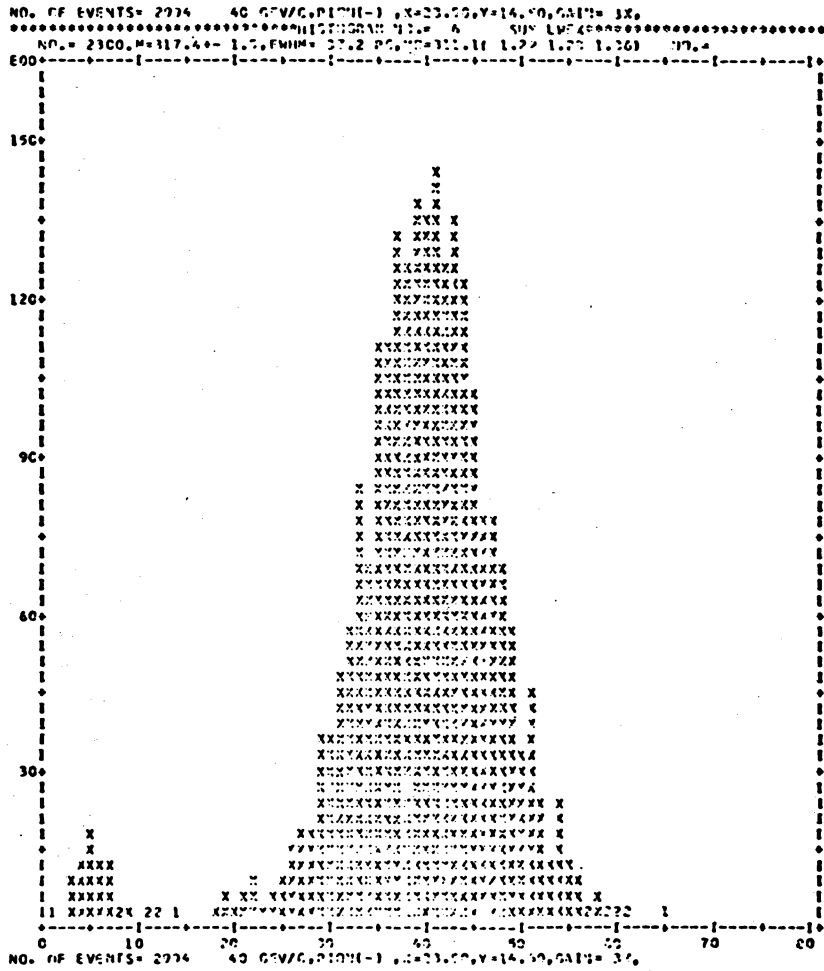
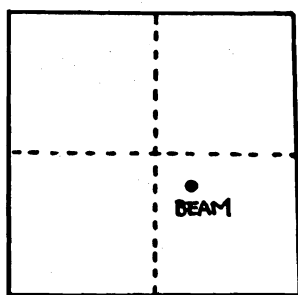
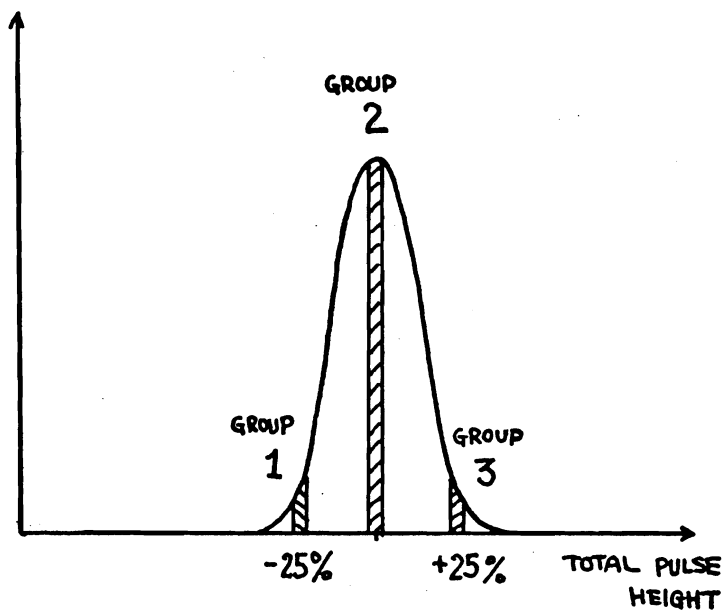


Fig. 6

100 GeV/c π^- (FWHM ~ 30%)



FRONT VIEW

Fig. 8

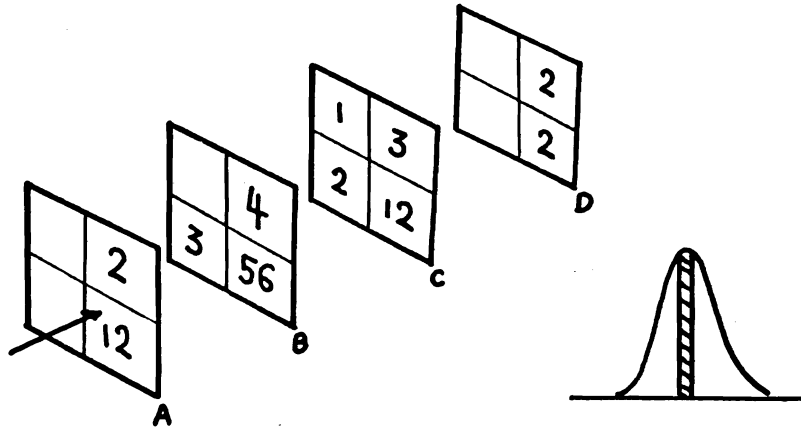


Fig. 9

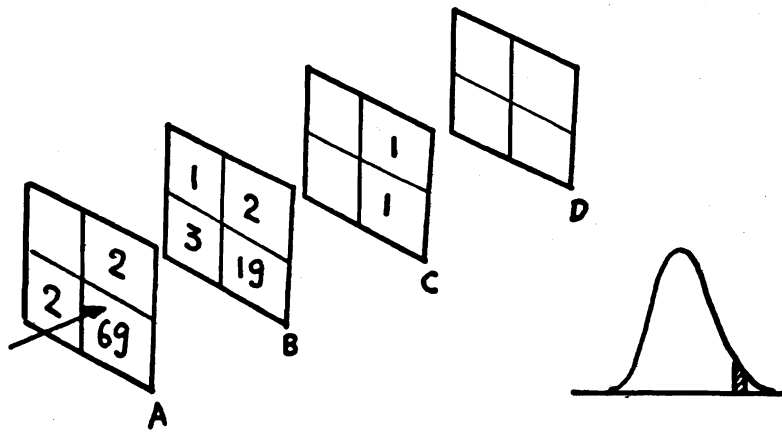


Fig. 10

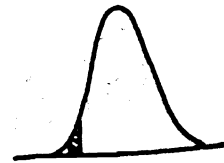
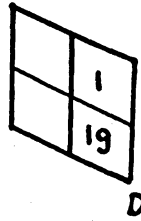
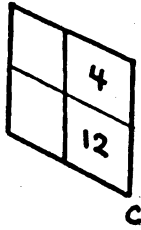
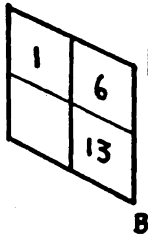
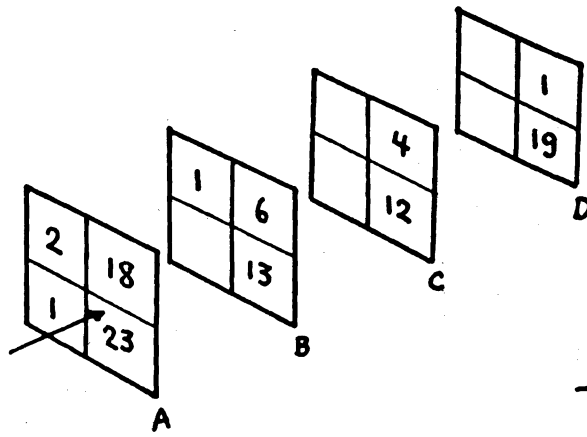
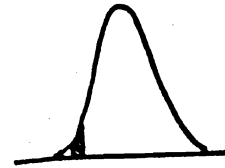
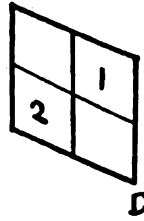
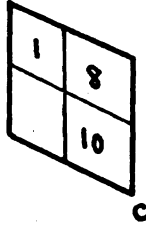
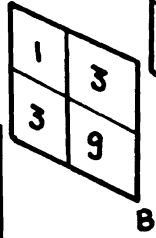
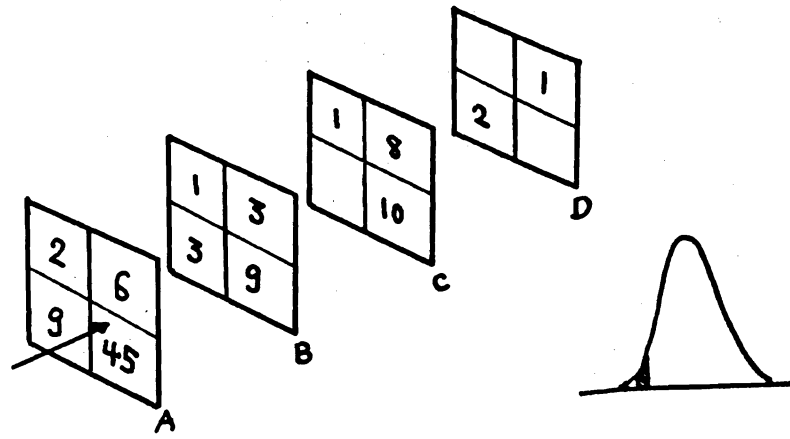


Fig. 11

100 GeV/c

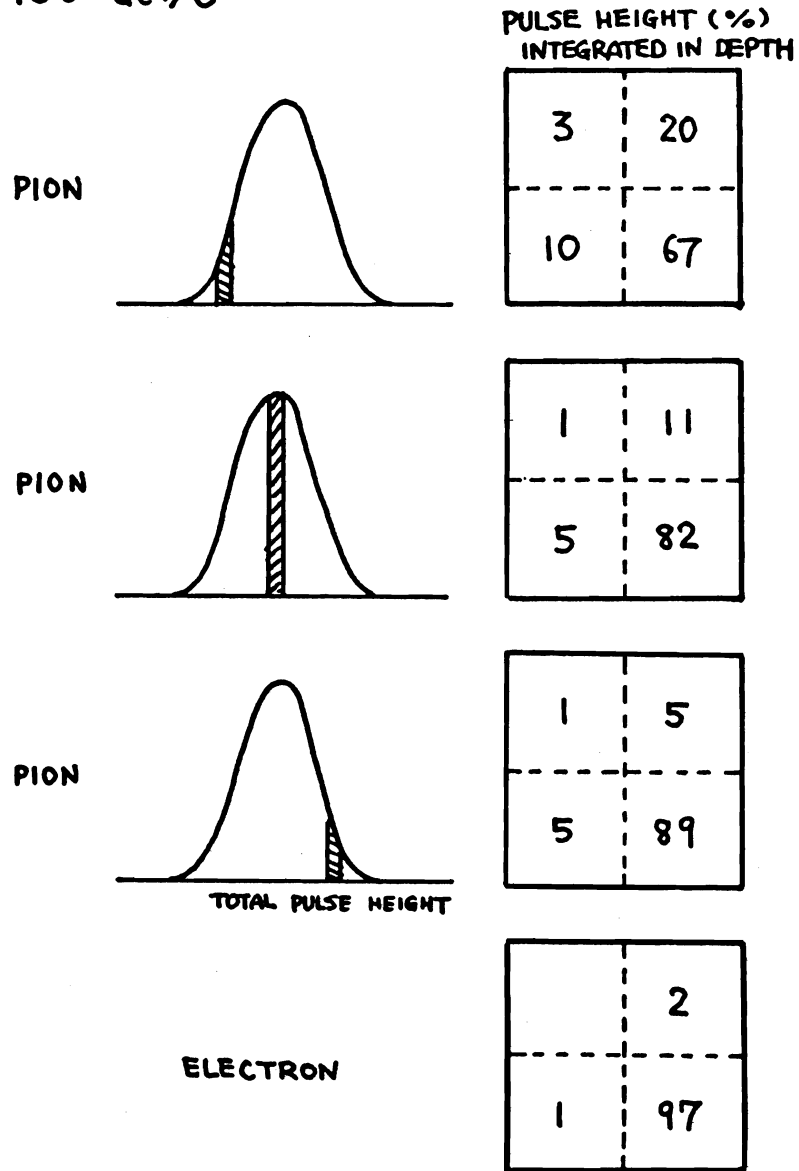


Fig. 12

200 GeV/c π^-

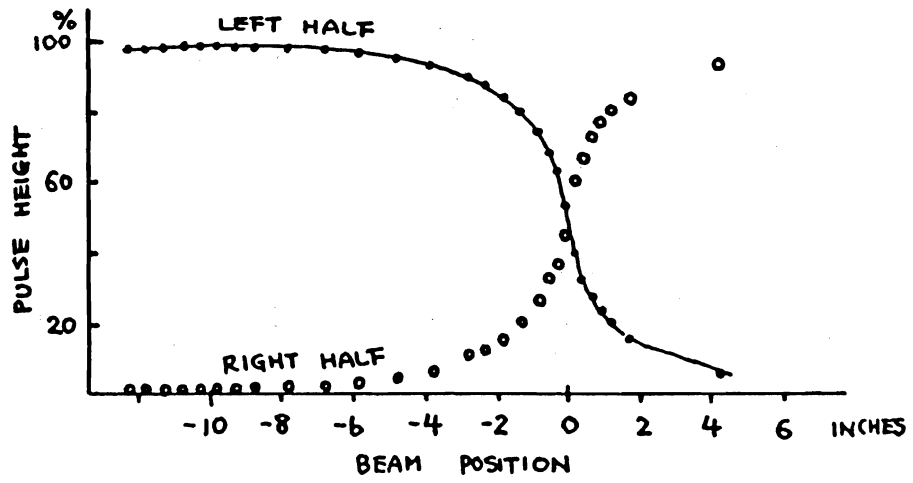
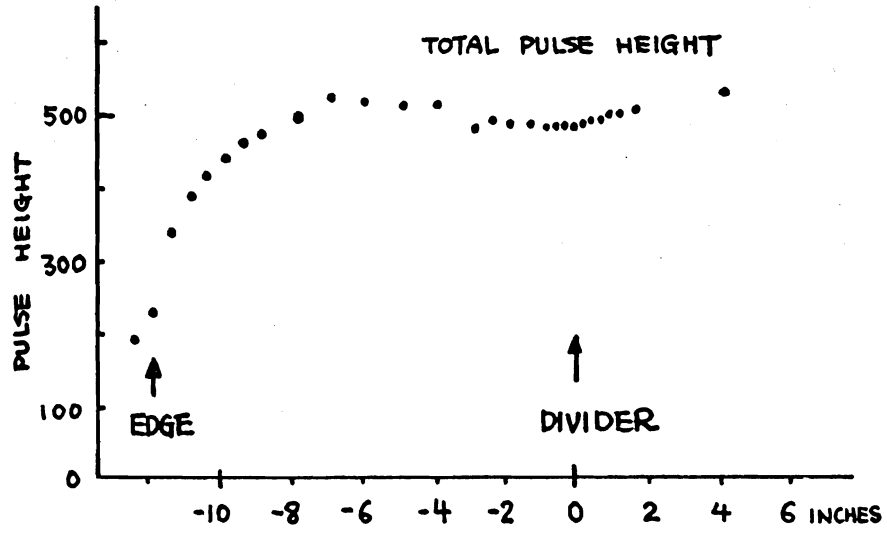


Fig. 13

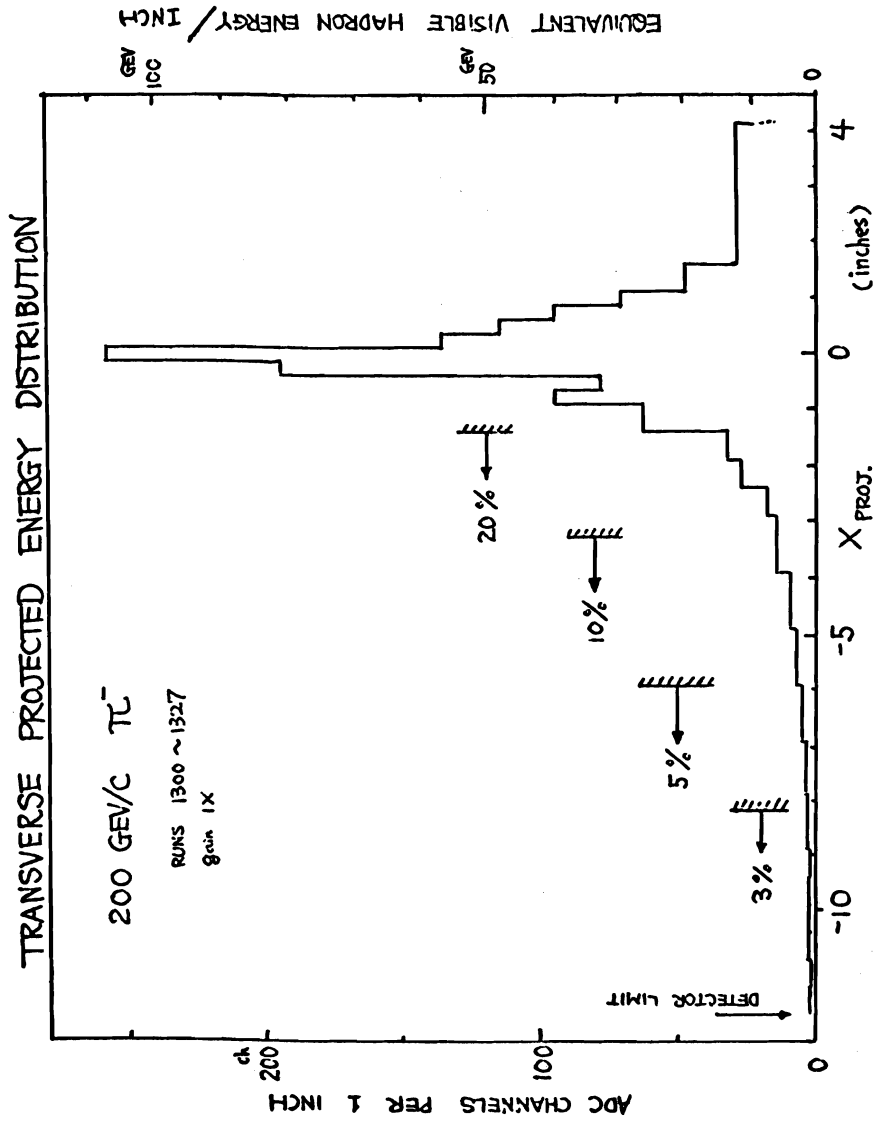
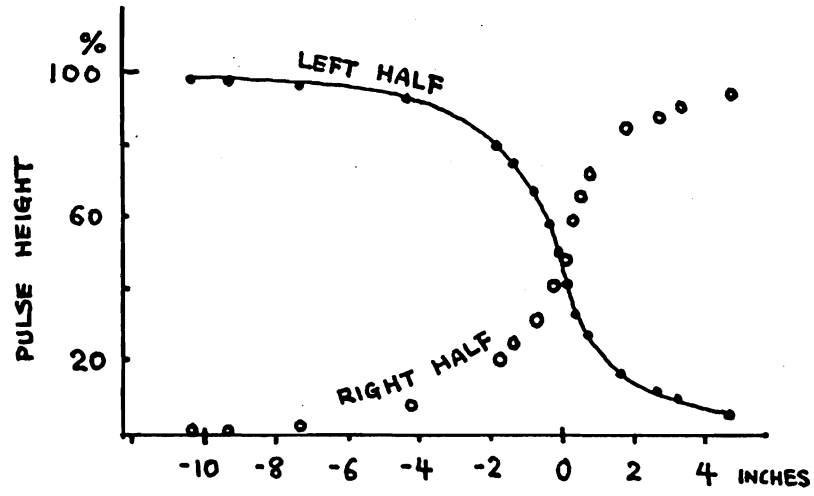


Fig. 1/4

(a) 20 GeV/c PION



(b) 20 GeV/c ELECTRON

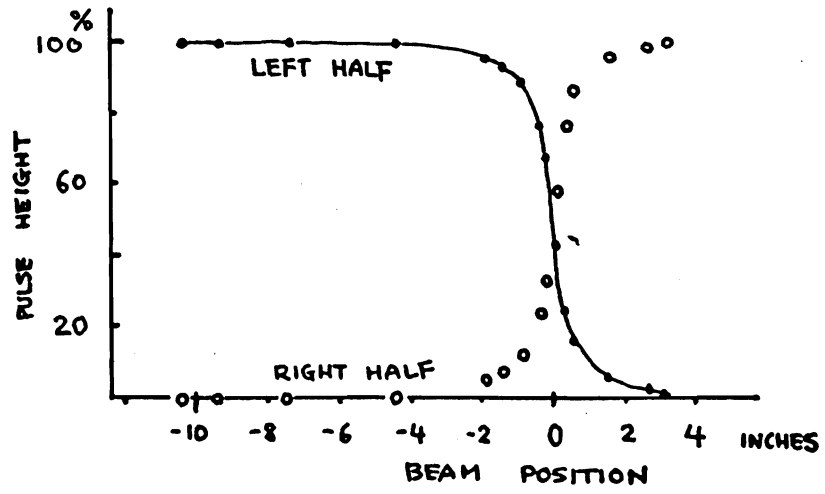


Fig. 15